IEEE Photonics Journal
An IEEE Photonics Society Publication

Open Access

Investigation of Ultrasmall 1 × *N* AWG for SOI-Based AWG Demodulation Integration Microsystem

Volume 7, Number 6, December 2015

Hongqiang Li
Wentao Gao
Enbang Li
Chunxiao Tang

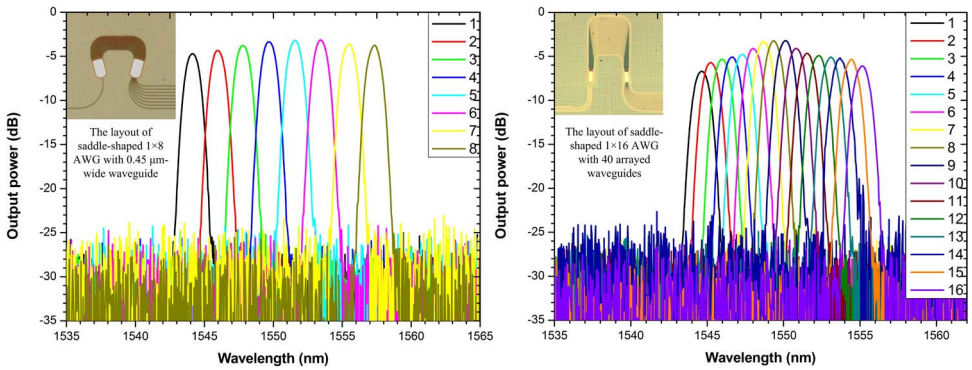

DOI: 10.1109/JPHOT.2015.2501678
1943-0655

Investigation of Ultrasmall 1 × *N* AWG for SOI-Based AWG Demodulation Integration Microsystem

Hongqiang Li,[1] Wentao Gao,[1] Enbang Li,[2] and Chunxiao Tang[1]

[1] School of Electronics and Information Engineering, Tianjin Polytechnic University, Tianjin 300387, China
[2] School of Physics, Faculty of Engineering, University of Wollongong, Wollongong, NSW 2522, Australia

DOI: 10.1109/JPHOT.2015.2501678

Manuscript received October 15, 2015; revised November 5, 2015; accepted November 12, 2015. Date of publication November 18, 2015; date of current version December 3, 2015. This work was supported in part by the National Natural Science Foundation of China under Grant 61177078, Grant 61307094, and Grant 31271871; by the Specialized Research Fund for the Doctoral Program of Higher Education of China under Grant 20101201120001; by the Tianjin Research Program of Application Foundation and Advanced Technology under Grant 13JCYBJC16800; and by the Science and Technology Development Foundation of University in Tianjin under Grant 20120609. Corresponding author: H. Li (e-mail: lihongqiang@tjpu.edu.cn).

Abstract: Optoelectronic integration technologies based on silicon-on-insulator (SOI) can bring revolutionary change to on-chip arrayed waveguide grating (AWG) demodulation systems. In this study, we present several ultrasmall 1 × *N* AWGs for an SOI-based AWG demodulation integration microsystem of different scales. The core sizes of the fabricated AWGs are smaller than 400 × 600 μm^2. Experimental results match the simulation results, indicating that AWGs have a good transmission spectrum of low crosstalk below −20 dB and low insertion loss below −6.5 dB. The fabricated AWGs can be perfectly applied to improve the integration level and performance of the SOI-based AWG demodulation integration microsystem.

Index Terms: Arrayed waveguide grating (AWG), silicon-on-insulator (SOI), optoelectronic demodulation integration microsystem.

1. Introduction

The monitoring of dynamic signals is important in medical applications and engineering safety. Fiber bragg grating (FBG) sensors have been gaining attention because of their significant advantages over conventional electrical sensors. Many challenging measurement problems have been addressed by FBG sensors, which have been commercially exploited for distributed strain and temperature measurement. We have previously studied and demonstrated a wearable optical fiber grating-based sensor for human body temperature measurement in the form of intelligent clothing [1]. However, the large size, high price, and discrete components of FBG demodulation systems limit the popularization and application of FBG sensing technology [2], [3]. Numerous FBG demodulation methods have been proposed, such as demodulation methods based on dynamic matched grating filtering, FBG demodulation methods based on Fabry-Polo (F-P) filter, and demodulation methods combining FBG and Mach-Zehnder Interferometers [4]–[6]. Currently, the AWG demodulation method gained attention because of the high precision of demodulation. AWG provides channels for optical demodulation as a wavelength division demultiplexer. The performance of AWG can directly determine the efficiency

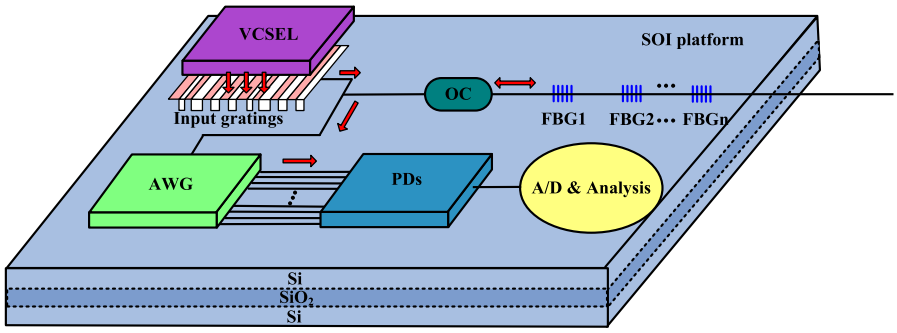

Fig. 1. Schematic diagram of the AWG demodulation integration microsystem.

of FBG sensors because it plays an important role in the AWG demodulation integration microsystem. However, the traditional AWG is too large to satisfy the initial requirements for discrete devices, including a compact structure, energy efficiency, and cost-effective on-chip communications. Thus, AWGs that fit the AWG demodulation integration microsystems, both in size and performance, are urgently required. The compact size of AWG can be achieved on a SOI-based platform because of its ultra-high relative refractive index difference Δ in the Si core and low index claddings. These characteristics allow sharp bends, micrometer-scale size, and easily enlarged scale integration of structures with other devices in the microsystem [7]. In 2011, Yang proposed a 48 $\times$ 48 AWG on SOI platform with 0.8 nm channel spacing. The fabricated AWG has a very compact size of about 220 $\times$ 470 μm^2, and the insertion loss and crosstalk is less than −4 dB and −15 dB, respectively [8]. Pathak demonstrated 12 ultra-small 400-GHz AWG channels on SOI with flattened spectral response using a multimode interference (MMI) mode shaper in 2011. Insertion loss and crosstalk are −3.29 dB and −17.0 dB, respectively, and device size is 560 $\times$ 350 μm^2 [9]. An 8 $\times$ 8 silicon nanowire AWG shows a crosstalk of about −17 dB and insertion loss of about −2.92 dB. These values were proposed by Wang Jing in 2014, with a 0.8-nm channel spacing footprint of only 730 $\times$ 300 μm^2 [10]. A 16-channel AWG on SOI platform is proposed by Pei in 2015, with crosstalk and insertion loss of −10 dB and −9.1 dB, respectively and a footprint size of 2900 $\times$ 1100 μm^2 [11]. Thus, the fabrication of high-performance AWGs with small sizes on SOI platform remains a challenge.

Several ultra-small 1 $\times$ N AWGs with a central wavelength of 1550 nm are fabricated to improve the integration level and performance of our SOI-based AWG demodulation integration microsystem. We optimized the structure of AWGs to achieve the best comprehensive quality through simulation results. The performance of the designed AWGs was analyzed by comparing simulation and experimental results in terms of insertion loss, crosstalk, and nonuniformity.

2. Device Design and Simulation

The AWG demodulation integration microsystem in a chip is composed of a 1550 nm vertical-cavity surface-emitting laser (VCSEL), an input gratings, an optical coupler, an AWG, several photoelectric detectors (PDs), several FBGs, and a system for analog-to-digital converting and analysis are as shown in Fig. 1. The VCSEL is interconnected on-chip. The optical port is exactly placed on the in-plane grating. The input gratings, optical coupler, and AWG are all etched on one SOI wafer; therefore; the device has a compact structure, good device integration, and lower cost for the optical path.

The light from the VCSEL irradiates vertically to the grating coupler and diffracts into the 2 $\times$ 2 coupler's input waveguide, then penetrates the FBG and AWG through the coupler. The reflected light of FBG also penetrates the AWG through the coupler. In case of influence from other AWG channels, the central wavelength of each FBG must be in the middle of the central wavelengths of two certain AWG adjacent channels (see Fig. 2). When the related variables affecting the spectrum of FBG change, the spectrum will shift and its overlap will alter with each AWG

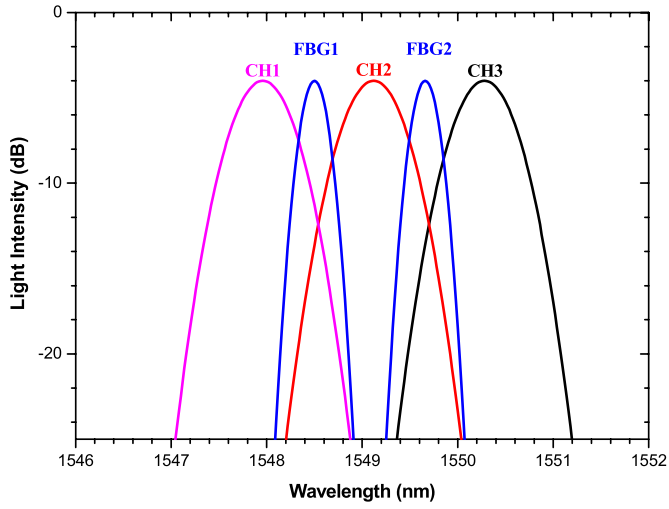

Fig. 2. Two FBG spectra along with the spectrum from three AWG channels.

TABLE 1

Parameters of designed 1 × 8 and 1 × 16 AWGs

	AWG(1×8)	AWG(1×16)
Diffraction order	45	30
$\Delta L(\mu m)$	30	25
No. of arrayed waveguides	24	35, 40
Free Spectral Range (nm)	60	31
Width of the waveguide (μm)	0.35, 0.4, 0.45, 0.5	0.4
Channel spacing (nm)	2	0.8

channel, causing a change in the light intensity measured at each channel. Each adjacent AWG channel can be used to demodulate the variables.

AWG is composed of 2N + 1 input rectangular waveguides, 2N + 1 output rectangular waveguides, two focusing slabs, and arrayed waveguide gratings that contain 2M + 1 waveguides, all of which are integrated onto the same substrate of silicon. We denote d as the arrayed waveguides separation, ΔX as output waveguides separation, ΔL as the path length difference of adjacent arrayed waveguides, m as the diffraction order, λ and λ_0 as the wavelength and central wavelength in free-space, respectively, and $\Delta\lambda$ as the wavelength spacing.

When multiplied light (the light source of C band with central length of 1550 nm) is launched into the input waveguide, the light is diffracted in the input slab and coupled into the arrayed waveguide. Each arrayed waveguide is located on a circle whose center is located at the end of the center input waveguide. The diffracted light enters the arrayed waveguides in the same phase. The arrayed waveguides have a constant path length difference ΔL between adjacent waveguides, and thus, lights of different wavelengths can attain the same phase difference at the exit of the waveguide. This phase difference results in wavelength-dependent wave-front tilting, and the lights with different wavelengths will then focus on each output waveguide.

We optimized the structure of AWG by designing different waveguide widths and shapes to obtain the proper parameters for high-performance AWG. Some parameters of the AWGs are shown in Table I. We designed eight kinds of 1 × 8 AWGs with different waveguide widths and structure shapes, as well as four kinds of 1 × 16 AWGs with different sizes and structure shapes. The larger-sized 1 × 16 AWGs are designed into more arrayed waveguides to decrease the insertion loss slightly increase the crosstalk.

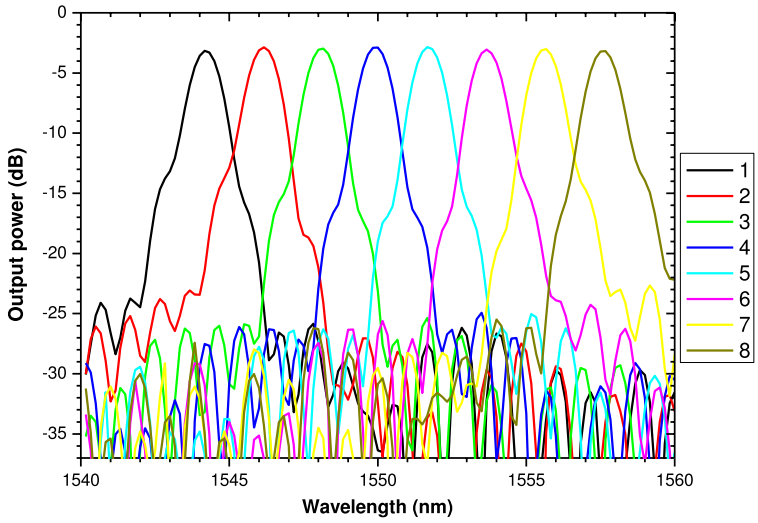

Fig. 3. Simulation results of the saddle-shaped 1 × 8 AWG with waveguide width of 0.45 μm.

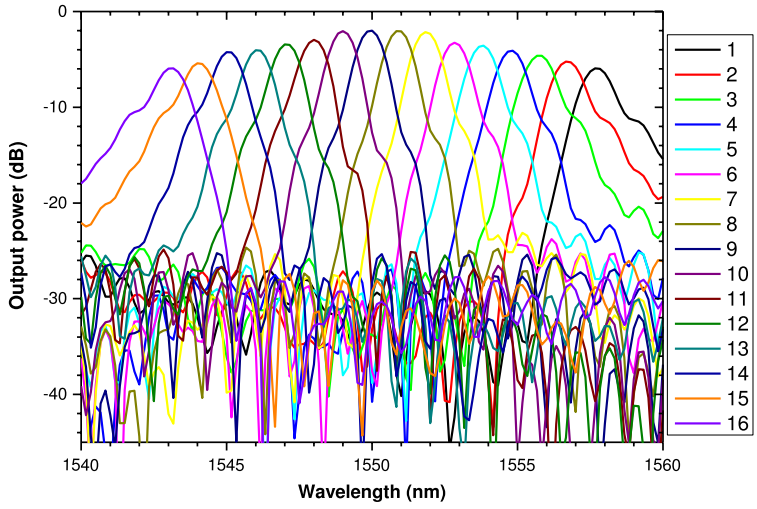

Fig. 4. Simulation results of saddle-shaped 1 × 16 AWG with 40 arrayed waveguides.

The parameters are amended in the simulation process. The simulated spectral responses of two AWGs are shown in Figs. 3 and 4. For the 1 × 8 AWGs, the saddle-shaped AWG with 0.45 μm waveguide width exhibits the best transmission spectrum (Fig. 3). From the simulation results, we can conclude that insertion loss is about −3.4 dB, nonuniformity is below 0.4 dB, and crosstalk is below −25 dB. For the 1 × 16 AWGs, the saddle-shaped AWG with 40 arrayed waveguides exhibited the best simulation results (Fig. 4). Insertion loss is about −5 dB, nonuniformity is 2.5 dB, and crosstalk is below −21 dB. Despite the small size, a good spectral response is achieved at a low crosstalk level and low insertion loss.

3. Device Fabrication and Experiment

Based on the comprehensive optimal design shown above, the designed AWGs and integration system were fabricated by IME in Singapore. These devices were fabricated on SOI wafer with 220-nm-thick top silicon layer, 2000-nm-thick buried SiO_2 layer and 2000-nm-thick substrate

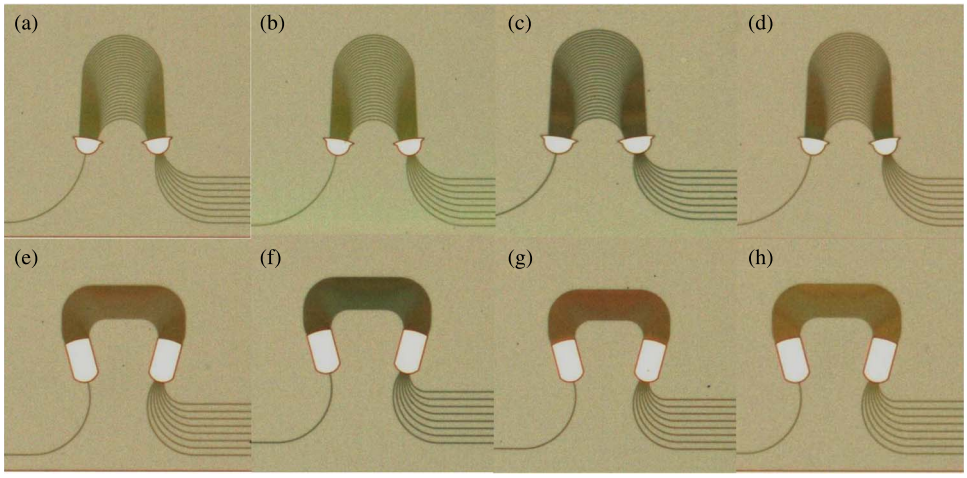

Fig. 5. Schematic layout of the microscope photo of eight fabricated 1 × 8 AWGs with different shape and width of the waveguide w. Tradition shape: (a) $w_1 = 0.35$ μm, (b) $w_2 = 0.4$ μm, (c) $w_3 = 0.45$ μm, (d) $w_4 = 0.5$ μm. Saddle shape: (e) $w_5 = 0.35$ μm, (f) $w_6 = 0.4$ μm, (g) $w_7 = 0.45$ μm, (h) $w_8 = 0.5$ μm.

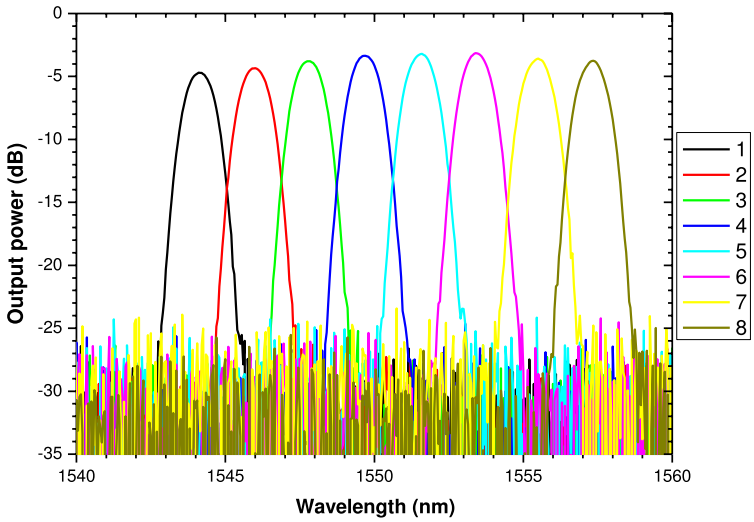

Fig. 6. Experiment results of saddle-shaped 1 × 8 AWG with waveguide width of 0.45 μm.

Si layer. We tested these devices in our laboratory. Fig. 5 shows the schematic layout of the microscopic photo of the eight fabricated 1 × 8 AWGs with different waveguide widths and shapes. We also found that the saddle-shaped AWG with 0.45 μm-wide waveguide exhibited the best transmission spectra (see Fig. 6). Core size is 270 × 380 μm^2. The saddle-shaped AWG exhibits a central channel loss of –3.18 dB, nonuniformity of 0.8 dB, and crosstalk level of –23.1 dB.

Fig. 7 shows the schematic layout of the microscopic photo of four fabricated 1 × 16 AWGs with different number of arrayed waveguides and shape. After the tests, we found that the saddle-shaped AWG with 40 arrayed waveguides exhibit good transmission spectrum (Fig. 8). We also found that the total insertion loss and crosstalk is below –5.5 dB and –21.4 dB, respectively, and that nonuniformity is about 4.3 dB. Core size is only 400 × 430 μm^2.

The differences between the simulation and experimental results in the crosstalk and insertion loss are caused by fabrication errors of the waveguides. These errors enlarged the phase errors

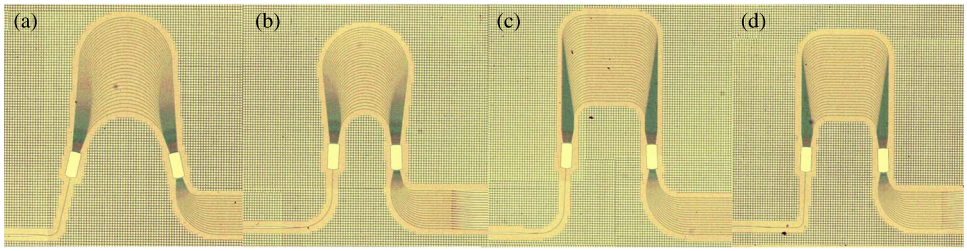

Fig. 7. Schematic layout of the microscopic photo of the four fabricated 1 × 16 AWGs with different number n of arrayed waveguides and shape. Tradition shape: (a) $n_1 = 40$, (b) $n_2 = 35$. Saddle shape: (c) $n_3 = 40$, (d) $n_4 = 35$.

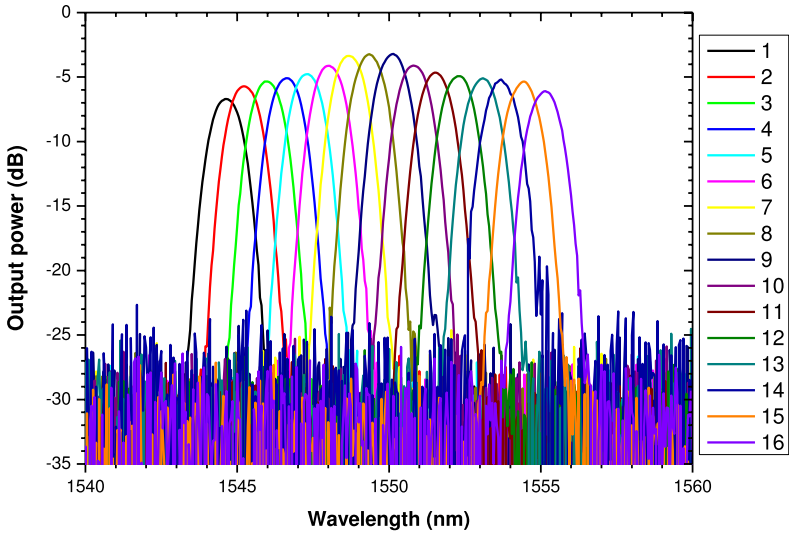

Fig. 8. Experiment results of saddle-shaped 1 × 16 AWG with 40 arrayed waveguides.

of the transmitted light, causing increased insertion loss and crosstalk. However, the device has also achieved expected performances in terms of size, crosstalk, nonuniformity, and insertion loss. Data obtained indicate that simulation results match the experiment results. We conducted a comparison between our proposed AWGs and the AWGs of recent studies on SOI, as shown in Table II. Our designed AWGs have great advantages, both in compact size and performances.

We have completed the testing of 1 × 8 and 1 × 16 AWGs as separate devices and as part of the integration system. We have also designed and fabricated four kinds of 1 × 32 AWGs, which were fabricated with different numbers of arrayed waveguides and shapes (see Fig. 9). Further tests are currently being conducted.

4. Conclusion

The design, fabrication, and measurement of two ultra-small 1 × N AWG have been presented. Low loss and crosstalk have been achieved through the optimal structure design. Results of the experiment show that the low insertion loss, crosstalk, and nonuniformity of the two designed AWGs can meet the requirements of the integrated arrayed waveguide grating demodulation system. The designed AWGs offer different demodulation channels for the integration system of different scales. The ultra-small 1 × N AWG for SOI-based arrayed waveguide grating demodulation integration microsystem was successfully demonstrated.

TABLE 2

Comparison of recent researches

AWG of recent researches	Crosstalk (dB)	Insertion loss (dB)	Core size (μm^2)
Our proposed 1×8 (2nm)	-23.1	-3.18	250×350
Our proposed 1×16(0.8nm)	-21.4	-5.5	400×430
48×48(0.8nm) [8]	-15	-4	220×470
1×12(0.8nm) [9]	-16.9	-3.29	560×350
8×8(0.8nm) [10]	-17	-2.92	730×300
1×16(0.8nm) [11]	-10	-9.1	2900×1100

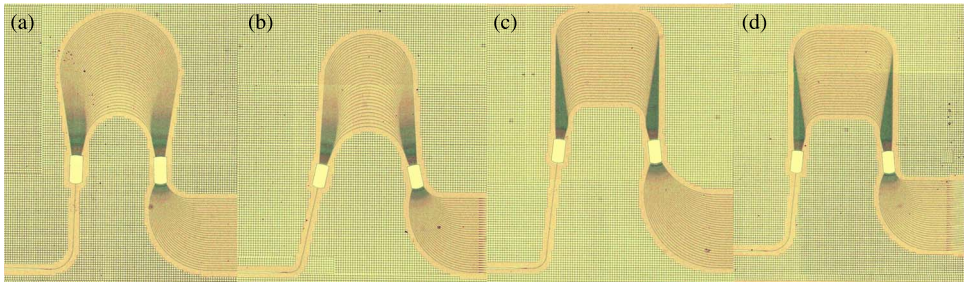

Fig. 9. Schematic layout of the microscopic photo of the four fabricated 1 × 32 AWGs with different number *n* of arrayed waveguides and shape. Tradition shape: (a) $n_1 = 40$, (b) $n_2 = 35$. Saddle shape: (c) $n_3 = 40$, (d) $n_4 = 35$.

We intend to design, fabricate, and test 1 × 64 and 1 × 128 AWGs to obtain better AWG performance, while maintaining its compact size and wider applicability for different sizes on FBG sensors. Increasing the performance of FBG sensors in different scales would be highly beneficial.

References

[1] H. Li, H. Yang, E. Li, Z. Liu, and K. Wei, "Wearable sensors in intelligent clothing for measuring human body temperature based on optical fiber Bragg grating," *Opt. Exp.*, vol. 20, no. 11, pp. 11740–11752, May 2012.
[2] Y. Zhao and Y. Liao, "Discrimination methods and demodulation techniques for fiber Bragg grating sensors," *Opt. Lasers Eng.*, vol. 41, no. 1, pp. 1–18, Jan. 2004.
[3] W. Liang and Y. Huang, "Highly sensitive fiber Bragg grating refractive index sensors," *Appl. Phys. Lett.*, vol. 86, no. 15, pp. 151122–151123, Apr. 2005.
[4] P. Cheben *et al.*, "A high-resolution silicon-on-insulator arrayed waveguide grating micro-spectrometer with sub-micrometer aperture waveguides," *Opt. Exp.*, vol. 15, no. 5, pp. 2299–2306, Mar. 2007.
[5] J. Pan *et al.*, "Optimization of dynamic matched grating filtering demodulation drived by piezoelectric ceramic," *Acta Photonica Sinica*, vol. 39, no. 2, pp. 243–246, Feb. 2010.
[6] H. Gao *et al.*, "InGaAs spectrometer and F-P filter combined FBG sensing multiplexing technique," *J. Lightw. Technol.*, vol. 26, no. 14, pp. 2282–2285, Jul. 2008.
[7] Y. Jiang, W. Ding, P. Liang, L. Fu, and C. Wang, "Phase-shifted white-light interferometry for the absolute measurement of fiber optic Mach–Zehnder interferometers," *J. Lightw. Technol.*, vol. 28, no. 22, pp. 3294–3299, Nov. 2010.
[8] B. Yang *et al.*, "Compact arrayed waveguide grating devices based on small su-8 strip waveguides," *J. Lightw. Technol.*, vol. 29, no. 13, pp. 2009–2014, Jul. 2011.
[9] S. Pathak, E. Lambert, P. Dumon, D. Van Thourhout, and W. Bogaerts, "Compact SOI-based AWG with flattened spectral response using MMI," in *Proc. GFP*, 2011, pp. 45–47.
[10] J. Wang *et al.*, "Low-loss and low-crosstalk 8 × 8 silicon nanowire AWG routers fabricated with CMOS technology," *Opt. Exp.*, vol. 22, no. 8, pp. 9395–9403, Apr. 2014.
[11] P. Yuan, Y. Wu, Y. Wang, J. An, and X. Hu, "Monolithic integration of a 16-channel VMUX on SOI platform," *J. Semicond.*, vol. 36, no. 8, Jan. 2015, Art. ID 084005.